Published in final edited form as:
Dev Biol. 2008 April 15; 316(2): 524–537.

Identification of downstream genetic pathways of *Tbx1* in the second heart field

Jun Liao[1], **Vimla S. Aggarwal**[1], **Sonja Nowotschin**[1,*], **Alexei Bondarev**[1], **Shari Lipner**[2], and **Bernice E. Morrow**[1,†]

1*Department of Molecular Genetics, Albert Einstein College of Medicine, 1300 Morris Park Ave., Bronx, NY 10461, USA*

2*Department of Cell Biology, Albert Einstein College of Medicine, 1300 Morris Park Ave., Bronx, NY 10461, USA*

Abstract

Tbx1, a T-box transcription factor, and an important gene for velo-cardio-facial syndrome/DiGeorge syndrome (VCFS/DGS) in humans, causes outflow tract (OFT) heart defects when inactivated in the mouse. *Tbx1* is expressed in the second heart field (SHF) and is required in this tissue for OFT development. To identify *Tbx1* regulated genetic pathways in the SHF, we performed gene expression profiling of the caudal pharyngeal region in *Tbx1*$^{-/-}$ and wild type embryos. *Isl1*, a key marker for the SHF, as well as *Hod* and *Nkx2-6*, were downregulated in *Tbx1*$^{-/-}$ mutants, while genes required for cardiac morphogenesis, such as *Raldh2*, *Gata4*, and *Tbx5*, as well as a subset of muscle contractile genes, signifying myocardial differentiation, were ectopically expressed. Pan-mesodermal ablation of *Tbx1* resulted in similar gene expression changes, suggesting cell-autonomous roles of *Tbx1* in regulating these genes. Opposite expression changes concomitant with SHF-derived cardiac defects occurred in *TBX1* gain-of-function mutants, indicating that appropriate levels of *Tbx1* are required for heart development. When taken together, our studies show that *Tbx1* acts upstream in a genetic network that positively regulates SHF cell proliferation and negatively regulates differentiation, cell-autonomously in the caudal pharyngeal region.

Keywords

Tbx1; second heart field; VCFS/DGS; gene expression profiling

INTRODUCTION

The development of the cardiac outflow tract (OFT) is vulnerable to genetic and environmental insults resulting in morphological defects of the heart. OFT anomalies, including abnormal alignment or septation, account for ~30% of all cases of congenital heart disease (Kelly and Buckingham, 2002), some of which co-occur in genetic syndromes. Velo-cardio-facial syndrome/DiGeorge syndrome (VCFS/DGS) (DiGeorge, 1965; Shprintzen et al., 1978) is associated with OFT defects due to de novo hemizygous 1.5-3 million base pair (Mb) 22q11.2

†To whom correspondence should be addressed: Bernice E. Morrow, Department of Molecular Genetics, Albert Einstein College of Medicine, 1300 Morris Park Ave., Bronx, NY 10461, Email: morrow@aecom.yu.edu Phone: 718-430-4274, Fax: 718-430-8778.
*Present address: Developmental Biology Program, Sloan-Kettering Institute, 1275 York Avenue, New York, NY 10021, USA.

deletions (Morrow et al., 1995; Shaikh et al., 2000). Studies in the mouse have demonstrated that *Tbx1*, a member of T-box containing transcription factor family present within the 1.5 Mb 22q11.2 region, is required for OFT development (Jerome and Papaioannou, 2001; Lindsay et al., 2001; Merscher et al., 2001). Functional mutations in *TBX1* have been found in rare non-deleted patients with the syndrome as well (Paylor et al., 2006; Stoller and Epstein, 2005; Yagi et al., 2003).

Tbx1 is expressed in the non-neural crest derived mesoderm of the caudal pharyngeal region, which is part of the second heart field (SHF) (Hu et al., 2004; Xu et al., 2004). Unlike the first heart field (FHF) cells, which differentiate at the cardiac crescent stage and give rise to the atria and left ventricle of the heart, SHF cells differentiate later and give rise to the OFT, right ventricle and part of the atria (reviewed by Buckingham et al., 2005). Inactivation of *Isl1*, a LIM homeodomain transcription factor expressed in the SHF, resulted in failed formation of the OFT, right ventricle and most of the atria due to failed proliferation and migration of this population of cells (Cai et al., 2003). Thus, the SHF, via *Isl1*, contributes significantly to heart development.

Lineage tracing-experiments showed that the progeny of *Tbx1*-expressing cells in the SHF contribute to the OFT and right ventricle. In $Tbx1^{-/-}$ embryos, although *Tbx1*-traced cells are present normally in the SHF, the contribution to the OFT is lower than in wild type embryos (Xu et al., 2004). Cell proliferation is also modestly reduced in the SHF of $Tbx1^{-/-}$ embryos (Xu et al., 2004; Zhang et al., 2006). Tissue-specific inactivation of *Tbx1* in the SHF by Nkx2-5-Cre (Xu et al., 2004) or Mesp1-Cre (Zhang et al., 2006) resulted in a persistent truncus arteriosus (PTA) and ventricular septal defect (VSD), same as those in $Tbx1^{-/-}$ embryos.

Two fibroblast growth factor (Fgf) genes expressed in the SHF, *Fgf8* and *Fgf10* are hypothesized to act downstream of *Tbx1* in cardiovascular development (Hu et al., 2004; Vitelli et al., 2002b). Both genes are downregulated in the SHF of $Tbx1^{-/-}$ mutants, but surprisingly, $Fgf10^{-/-}$ embryos do not have OFT defects (Marguerie et al., 2006) nor did *Tbx1/Fgf8/Fgf10* triple heterozygous mice (Aggarwal et al., 2006), indicating that other genes are responsible for these defects. Recently, *Pitx2* was shown to act downstream of *Tbx1* in the early SHF, but *Tbx1/Pitx2* double heterozygosity affected only OFT alignment but not septation, and it occurred with reduced penetrance (Nowotschin et al., 2006).

It has been difficult to identify genes downstream of *Tbx1* in the SHF. Here, we report a systematic genome-wide search for genes regulated directly or indirectly by *Tbx1* in the caudal pharyngeal region containing the SHF. Our data show that global or pan-mesodermal inactivation of *Tbx1* disrupts a network of genes maintaining cell proliferation in the SHF and causes ectopic expression of known genes required for differentiation, whereas overexpression causes opposite expression changes of a subset of these genes. These findings for the first time delineate a potential molecular network downstream of *Tbx1*.

MATERIALS AND METHODS

Mouse mutants

Generation of $Tbx1^{+/-}$, BAC transgenic and $Tbx1^{flox/-}$ mice have been described previously (Arnold et al., 2006; Merscher et al., 2001). *T-Cre* transgenic mice (Perantoni et al., 2005) were obtained from Dr. Mark Lewandoski. A ROSA26 reporter strain (Soriano, 1999) was obtained from Jackson Laboratories. $Tbx1^{+/-}$ and BAC transgenic mice are congenic in the FVB genetic background. ROSA26 mice were maintained in the C57BL6 background. All the other strains were maintained in a mixed C57BL6/129 background.

Mouse embryo dissections

Mouse embryos in the FVB background at E8.75, E9.75 and E10.75 were isolated in cold PBS. Somite pairs were counted to define the stages: 10-12 pairs of somites were defined as E8.75; 23-25 pairs of somites were defined as E9.75 and 35-37 pairs of somites were defined as E10.75. The caudal pharyngeal region without the first pharyngeal arch and the neural tube was dissected and placed in RNAlater RNA stabilization reagent (QIAGEN) at 4 °C.

Total RNA preparation

To obtain enough RNA for the microarray hybridization experiments, dissected pharyngeal tissue from 5-10 embryos were pooled. The tissue was homogenized in Buffer RLT (QIAGEN). Total RNA was isolated with either RNeasy Mini Kit (QIAGEN) (for E9.75 and E10.75 tissue) or the RNeasy Micro Kit (QIAGEN) (for E8.75 tissue) according to the manufacturer's protocol. Quality and quantity of total RNA was determined using an Agilent 2100 Bioanalyzer (Agilent) and a ND-1000 Spectrophotometer (NanoDrop) respectively.

Target preparation

For total RNA isolated from E9.75 or E10.75 tissue, target preparation was carried out according to Affymetrix's One-Cycle Eukaryotic Target Labeling Assay. Specifically, using One-Cycle cDNA Synthesis Kit (Affymetrix), 1-5 μg total RNA was first reverse transcribed to obtain first-strand cDNA and then second-stranded cDNA was synthesized in an RNase H-mediated reaction. The double-stranded cDNA was purified with the Sample Cleanup Module (Affymetrix) and this served as a template in the subsequent *in vitro* transcription (IVT) reaction using the IVT Labeling Kit (Affymetrix). The resulting biotinylated cRNA targets were then cleaned up and fragmented with Sample Cleanup Module (Affymetrix).

For the E8.75 tissue, the biotinylated single-strand cDNA targets were amplified from 20-50 nanograms (ng) starting total RNA using The Ovation Biotin RNA Amplification and Labeling System (NuGEN).

Microarray processing

A total of 20 μg fragmented, biotin labeled cRNA (for E9.75 or E10.75 tissue) or 2.2μg cDNA (for E8.75 tissue) from the last step was hybridized to the GeneChip Test3 array (Affymetrix) to test the quality of the labeled target. Targets which passed the test were then hybridized to the GeneChip Mouse Genome 430A 2.0 Arrays (Affymetrix). Hybridization, washing, staining and scanning was performed in the AECOM Affymetrix Facility according to the Affymetrix manual.

Data analysis

GeneChip data were analyzed with ArrayAssist Lite (Stratagene). Briefly, the original Affymetrix GeneChip CEL files generated by the AECOM Affymetrix Facility were imported into ArrayAssist Lite and a master data table based on them was created by GC-RMA. Then the data was converted to logarithmic scale and the significance analysis was performed using two classes, unpaired *t*-test with a cut-off of fold change >2 and *p*-value <0.05.

Quantitative RT-PCR (qRT-PCR)

To obtain enough total RNA and minimize the variability of gene expression in individual embryos, each sample contained microdissected tissue from two to five embryos. Total RNA was isolated using the RNeasy Protect Mini Kit (Qiagen), and used for the first-strand cDNA synthesis with SuperScript First-Strand Synthesis System for RT-PCR (Invitrogen). The PCR reactions were performed in the LightCycler apparatus (Roche) using LightCycler-FastStart DNA Master SYBR Green I (Roche). All values were normalized to the level of *Gapdh*, which

was used as an internal control in each sample. For each experimental group, three to five samples were tested and the average of them was calculated. Statistical significance between different groups was calculated by unpaired Student's *t*-test. Gene-specific primer pairs used for PCR amplification are listed in Table S4.

In situ hybridization (ISH)

Digoxigenin-labeled RNA probes for *Tbx1* (Nowotschin et al., 2006), *Tbx5* (Chapman et al., 1996), *Gata4*, *Isl1* (Cai et al., 2003), and *Nkx2-5* (Lyons et al., 1995) were prepared by standard methods (Roche). All the other probes were amplified by PCR from either mouse genomic DNA or cDNA, using the primers listed in Table S5. All forward primers contained T3 polymerase priming sequence and all reverse primers contained T7 polymerase priming sequence. The PCR product was purified by the PCR Purification Kit (Qiagen), and anti-sense RNA was in vitro transcribed and labeled with the T7 RNA polymerase (Roche) and DIG RNA Labeling Mix (Roche), using the Digoxigenin labeling method. Digoxigenin-labeled RNA probes were purified with mini Quick Spin RNA Columns (Roche). Whole mount in situ hybridization was performed as previously described (Nowotschin et al., 2006). To generate histological sections, embryos following whole mount in situ hybridization were dehydrated through a graded ethanol series (70% EtOH for 5 minutes, 95% EtOH for 10 minutes, 2 times 100% EtOH for 5 minutes, 100% EtOH for 10 minutes, 2 times Xylene for 15 minutes), embedded in paraffin wax and sectioned at a thickness of 10 μm in a microtome.

Histology

Mouse embryos were dissected in PBS (Mediatech) and fixed in 10% neutral buffered Formalin solution (Sigma) overnight. They were dehydrated through graded ethanol, embedded in paraffin and sectioned (7-10 μm) using a microtome.

In silico promoter analysis

The annotated mouse genomic sequences for *Raldh2*, *Hod*, and *Nkx2-6* were examined for regions conserved among mammalian species (July 2007 Assembly; UCSC Genome Browser http://genome.ucsc.edu/). Most conserved blocks were located within 10 kb upstream or downstream of exons of the three. We searched for T-box binding sequences within each of the gene loci. The consensus sequences were fully conserved in mouse, rat, and human genomic DNA.

RESULTS

Expression profiling of the caudal pharyngeal apparatus in *Tbx1*$^{-/-}$ mutants

To identify genes that act downstream of *Tbx1* in the SHF, the caudal pharyngeal region was microdissected at E8.75 (10-12 somites), E9.75 (23-25 somites) and E10.75 (35-37 somites; see Fig. S1A in the supplementary material), in both wild type and *Tbx1*$^{-/-}$ embryos. The three stages, coincident with highest *Tbx1* expression levels, should provide a complete set of *Tbx1*-dependent genes. By quantitative measurements, we found the morphology of caudal pharyngeal region of *Tbx1*$^{-/-}$ embryos was grossly normal at E8.75, though morphological defects due to hypoplasia of the caudal pharyngeal arches were observed at E9.75 and E10.75 (see Fig. S2 in the supplementary material). Labeled targets from three independent pools of RNA samples were hybridized to Affymetrix arrays, containing over 14,000 known mouse genes. With the criteria of fold change >2 and p-value < 0.05, 120, 89, and 113 probe sets were identified for stages of E8.75, E9.75, and E10.75 respectively (see Tables S1, S2, S3 in the supplementary material). The candidates included genes of all classes (Gene Ontology categories, GO; see Fig. S1B in the supplementary material). This analysis revealed some notable trends including a decrease in expression of genes encoding signaling molecules and

increase in expression of genes encoding structural proteins, over time (see Fig. S1B in the supplementary material). Visible inspection of the gene lists (see Tables S1, S2, S3 in the supplementary material) revealed a strikingly large set of genes required for heart development altered in the mutant embryos, despite the fact that the heart was removed from the microdissected tissue (see Fig. S1A in the supplementary material).

The number of genes shared by different stages is summarized in a Venn diagram (see Fig. S1C in the supplementary material). Comparison of the gene lists revealed that some are shared by E8.75 and E9.75 or E9.75 and E10.75, but only two genes, *Raldh2* (retinaldehyde dehydrogenase type 2, also named *Aldh1a2*) and *Cpa1* (carboxypeptidase A1) were shared among all three stages, indicating a highly dynamic gene expression profile regulated by *Tbx1* during pharyngeal development. Morphology alterations at E9.75 and E10.75 could also have accounted for some of the gene expression changes.

Validation of selected candidate genes

Many of the genes found have important functions in cardiac development, but were not previously linked to the SHF or *Tbx1*. Genes with potential direct relevance to the SHF are listed in Table 1. Some of these genes were chosen for further validation by qRT-PCR and ISH (Table 1). Three new pools of wild type and *Tbx1*$^{-/-}$ embryo tissue were tested for each stage by qRT-PCR and p-values were calculated. Unlike the microarray experiments, all the samples for qRT-PCR analysis were prepared in the same way, making it possible to directly compare expression levels of candidate genes at all three stages. In both qRT-PCR and ISH experiments, *Nkx2-5* served as a negative control because of its unchanged expression in the SHF of *Tbx1* null embryos, while *Raldh2* served as a positive control because its ectopic expression in the pharyngeal apparatus of *Tbx1*$^{-/-}$ embryos has been reported at later stages (Guris et al., 2006;Ivins et al., 2005). As a prelude to ISH studies, the expression pattern of *Tbx1* was assessed in detail and compared with those of selected genes. Co-expression with *Tbx1* in the SHF was a determining factor for further analysis at multiple stages.

Hod, *Isl1*, and *Nkx2-6* are downregulated in the SHF of *Tbx1*$^{-/-}$ embryos

Hod, also named *Hop*, encodes an unusual homeobox domain only protein expressed in the linear heart tube and SHF, required for forming the ventricular myocardium (Chen et al., 2002; Shin et al., 2002). We found that *Hod* was downregulated 2.11 fold at E8.75 by microarray analysis (Table 1), and confirmed by qRT-PCR analysis (Fig. 1A). ISH results from E8.5, E8.75, and E9.0 showed that *Hod* is expressed in both the pharyngeal arch core mesoderm and the SHF in wild type embryos (Fig. 1B,E,H), overlapping with *Tbx1* expression (Fig. 1D,G). In contrast to the wild type embryos, *Hod* expression was not visible by whole mount ISH in *Tbx1*$^{-/-}$ embryos at E8.5 (Fig. 1C). At E8.75, *Hod* expression was only observed in the pharyngeal arch core mesoderm, especially in the first arch mesoderm, but not in the SHF in *Tbx1*$^{-/-}$ embryos (Fig. 1F). At E9.0, *Tbx1*$^{-/-}$ embryos only showed *Hod* expression in the cranial part of SHF but not caudal part (Fig. 1I). Although there was a clear downregulation at E8.75, no significant difference in *Hod* expression between wild type and *Tbx1*$^{-/-}$ embryos was observed after E9.75 by qRT-PCR (Fig. 1A). These results suggest that *Tbx1* may be required for activation of *Hod* at the earliest stages of pharyngeal development, but not for its maintenance later on.

Isl1 is the key marker for the SHF and is required for OFT development (Cai et al., 2003). Inactivation of *Isl1* results in major looping and OFT defects with missing segments of the heart (Cai et al., 2003). *Isl1* expression was decreased 2.4 fold by microarray analysis and 2.08 fold by qRT-PCR in E8.75 *Tbx1*$^{-/-}$ embryos (Table 1; Fig. 1A). ISH from E8.5 and E9.0 showed downregulation of *Isl1* in the caudal part of the SHF of *Tbx1*$^{-/-}$ embryos (Fig. 1J-O), suggesting precise spatial and temporal regulation by *Tbx1*. There was no change in the pattern of *Isl1*

expression in the pharyngeal endoderm in the same region, which is another domain of co-expression with *Tbx1* (Fig. 1J-O).

The *Nkx2-6* gene belongs to the same *NK-2* homeobox gene family as *Nkx2-5* and they have overlapping expression patterns in the pharyngeal endoderm and SHF (Biben et al., 1998; Nikolova et al., 1997). While *Nkx2-5* was not changed, *Nkx2-6* was significantly downregulated in *Tbx1*$^{-/-}$ mutants at all three stages, with the greatest change at E8.75 (Table1), confirmed by qRT-PCR (Fig. 1A). ISH from E9.0 and E9.5 embryos showed that *Nkx2-6* expression in the SHF was significantly reduced in *Tbx1*$^{-/-}$ embryos, while its expression in the pharyngeal endoderm is unchanged (Fig. 1P,Q, and data not shown), similar to *Isl1*. Thus, *Hod*, *Isl1*, and *Nkx2-6* were downregulated in the caudal SHF of *Tbx1*$^{-/-}$ embryos at E8.5-E9.0. As expected, *Nkx2-5* expression was not changed in the SHF (Fig. 1R,S).

Ectopic expression of *Raldh2*, *Gata4* and *Tbx5* in the SHF of *Tbx1*$^{-/-}$ embryos

Numerous transcription factors form an interconnected network to regulate specification and myocardial differentiation of the heart (reviewed by Bruneau, 2002). Many of key genes in this network were ectopically expressed in *Tbx1*$^{-/-}$ embryos (Table 1). In particular, three genes important for myocardial differentiation, *Raldh2*, *Gata4*, and *Tbx5*, showed increased expression at multiple stages by microarray (Table 1) and qRT-PCR analysis at E8.75 and later (Fig. 2A). To determine whether upregulation of these three genes is specific to the SHF, ISH experiments were performed.

Radlh2 is an enzyme required for the synthesis of retinoic acid (RA), one of the earliest morphogens needed for the specification of linear heart tube (reviewed by Xavier-Neto et al., 2001). Previous studies of *Tbx1* mouse mutants showed ectopic expression of *Raldh2* in the pharyngeal mesoderm of *Tbx1*$^{-/-}$ embryos after E9.5, but it was not known whether the upregulation was due to gene activation or morphological alterations in these later stages (Guris et al., 2006; Ivins et al., 2005). ISH analysis showed that *Raldh2* was expressed in the caudal part of the SHF at E9.0 in wild type embryos (Fig. 2C,E). In contrast, *Raldh2* expression was expanded cranially at E9.0 in *Tbx1*$^{-/-}$ embryos (Fig. 2D,F). Since there was no detectable morphological difference between wild type and *Tbx1*$^{-/-}$ embryos at E9.0 (compare Fig. 2C and 2D, and also see Fig. S2 in the supplementary material), this indicates that ectopic expression of *Raldh2* is likely a direct result of the *Tbx1* null mutation and not secondary to morphological defects.

Gata4 is one of the earliest transcription factors expressed in the heart and is needed for activation of many myocardial differentiation genes (reviewed by Pikkarainen et al., 2004). There is a low level of *Gata4* expression in the SHF of wild type embryos at E9.0-E9.5 (Fig. 2G and data not shown), while in *Tbx1*$^{-/-}$ embryos, ectopic expression was found throughout the SHF region at E9.0 and more restricted to the cranial part of the SHF at E9.5 (Fig. 2H and data not shown).

Tbx5 haploinsufficiency is responsible for human Holt-Oram syndrome (Bruneau et al., 2001). Although *Tbx5*$^{-/-}$ mice have atrial and left ventricular defects, the OFT and right ventricle are normal, indicating that *Tbx5* is not required for the SHF development (Bruneau et al., 2001). ISH experiments also showed that *Tbx5* was expressed very weakly in the SHF of wild type embryos (Fig. 2I), but was expressed ectopically in the caudal SHF of *Tbx1*$^{-/-}$ embryos at E9.0 and E9.5 (Fig. 2J and data not shown), and as for the other genes, in regions containing *Tbx1* expressing cells (Fig. 2B). In contrast, *Hand1*, another gene expressed in the heart tube, did not show any ectopic expression in the SHF of *Tbx1*$^{-/-}$ embryos (Fig. 2K,L).

Ectopic expression of myogenic structural genes in the SHF

As the myocardial progenitor cells differentiate to cardiac muscle, specific muscle structural genes are expressed, such as myosins, actins, troponins, calponin, actinin and titin (reviewed by Franco et al., 1998). Since the heart itself was removed from the dissected tissues used for microarray analysis, increased expression of a large group of muscle contractile genes found by microarray in the homozygous null mutants, especially at E10.75, was unexpected (Table 1). We tested three of them, *Actc1* (alpha cardiac actin), *Myh6* (*α-MHC*, alpha myosin heavy chain), and *Myl7* (*Mlc2a*, atrial myosin light chain 2) by qRT-PCR. The results showed increased expression of *Actc1*, *Myh6*, and *Myl7* in *Tbx1*$^{-/-}$ embryos at the three stages examined, with the greatest changes detected at E8.75 (Fig. 3A). Differences in the ability to detect increased expression earlier in development by qRT-PCR rather than by microarray reflect enhanced sensitivity of the qRT-PCR approach.

ISH experiments were performed for *Myh6* at E9.0 and increased expression of *Myh6* was detected in the SHF of *Tbx1*$^{-/-}$ embryos (Figure 3C). These results demonstrate muscle differentiation marker genes were ectopically expressed in the SHF of *Tbx1*$^{-/-}$embryos.

Gene expression changes are cell autonomous

Tbx1 is expressed in both pharyngeal endoderm and mesoderm and both expression domains seem important for OFT development (Arnold et al., 2006; Zhang et al., 2006). Thus it is important to determine whether *Tbx1* expression in the SHF plays a cell-autonomous role in regulating above downstream genes in the SHF. For this question, we ablated *Tbx1* by crossing *Tbx1*$^{flox/-}$ mice (Arnold et al., 2006) with pan-mesodermal expressing T-Cre transgenic mice (Perantoni et al., 2005). Recombination occurred in mesoderm derived tissues including the SHF but not in the pharyngeal endoderm (see Fig. S3A in the supplementary material). We then assessed *Tbx1* expression in conditional null mutant embryos at E9.5 (see Fig. S3C in the supplementary material) and E10.5 (data not shown) to determine whether it was properly inactivated. We found that *Tbx1* was expressed normally in the pharyngeal endoderm as expected, and its expression was reduced in the mesodermal tissues but not eliminated (see Figure S3C in the supplementary material), indicating partial ablation. The embryos had hypoplastic 2nd, 3rd, and 4th pharyngeal arches (compare Fig. S3B with S3C in the supplementary material). These morphological defects were less severe than those in *Tbx1*$^{-/-}$ and Mesp1-Cre-mediated conditional mutants, which completely lacked the caudal pharyngeal arches (Liao et al., 2004; Zhang et al., 2006). However, as in the *Tbx1*$^{-/-}$ and *Mesp1-Cre* conditional mutants, all T-Cre-mediated conditional mutant embryos died at birth with a PTA and VSD (see Fig. S3D-G in the supplementary material), indicating that the *Tbx1* expression level was below the dosage threshold needed for normal outflow tract development in the pharyngeal mesoderm.

We examined the expression patterns of *Isl1*, *Nkx2-6*, *Raldh2*, *Tbx5* and *Gata4* in the SHF of these embryos at E9.0 or E9.5. As before, we found *Isl1* and *Nkx2-6* were downregulated (Fig. 4A-D), while *Raldh2*, *Tbx5* and *Gata4* were upregulated (Fig. 4E-J). Our data suggests that alteration of expression of these genes in the SHF is cell autonomous.

SHF-derived defects in *TBX1* gain-of-function mutants

We previously generated bacterial artificial chromosome (BAC) transgenic mice overexpressing four transgenes including *TBX1* (Funke et al., 2001; Merscher et al., 2001). These mice show reduced viability and malformations in the derivatives of the pharyngeal apparatus with variable expressivity. Most of these defects were rescued by crossing in the *Tbx1* null allele, indicating the important role of *Tbx1* dosage in the pharyngeal development (Liao et al., 2004). Occasionally intracardiac and OFT defects such as a VSD (Merscher et al., 2001), PTA, and a double outlet right ventricle (DORV) (Liao et al., 2004) were also found in

these mice. Here we performed more detailed histological studies of the transgenic mice at E17.5 (n = 12) than was previously done (Merscher et al., 2001). The most common heart defect (5 of 12 embryos) was a thinning of the myocardial wall in the right ventricle, especially in the region juxtaposed to the interventricular septum (Fig. 5B,G,H). In the most severe cases, a muscular VSD was present (data not shown). A membranous VSD, typical in VCFS/DGS, occurred in 3 out of 12 embryos (Fig. 5E,G). Interestingly, it was always present together with a DORV, but not necessarily with myocardial hypoplasia (Fig. 5F,H). In contrast, none of wild type embryos we checked (n = 5) had any of these defects (Fig. 5A,C,D). Since SHF cells contribute to endothelial and myocardial components of the OFT, right ventricle and ventricular septum (Verzi et al., 2005), most of these defects could be due to the abnormal development of the SHF resulting from increased *TBX1* dosage. We postulated that some of the genes found by microarray analysis may be altered in the transgenic embryos, and if so, it would further implicate their function in the SHF.

Opposite gene expression changes in *TBX1* gain-of-function mutants

To determine whether expression levels of the same genes that were altered in the *Tbx1*$^{-/-}$ mutant were also changed in the *TBX1* transgenic embryos, qRT-PCR studies were performed. Unlike *Tbx1*$^{-/-}$ mice, *TBX1* transgenic embryos do not have morphological changes in the pharyngeal apparatus (Liao et al., 2004), which makes them an ideal model to validate whether the expression changes observed in *Tbx1*$^{-/-}$embryos are morphology-independent. The expression levels of *Hod*, *Isl1*, *Nkx2-6*, *Raldh2*, *Tbx5*, *Gata4*, *Actc1*, and *Myh6* in the caudal pharyngeal apparatus of E8.75 *TBX1* transgenic embryos were assessed by qRT-PCR analysis. Among genes that were downregulated in *Tbx1*$^{-/-}$ embryos, *Nkx2-6* showed significantly increased expression in *TBX1* transgenic embryos (Fig. 5K), while three upregulated genes, *Raldh2*, *Tbx5*, and *Gata4* showed significantly decreased expression (Fig. 5K). There was a reduced area of *Raldh2* expression in the SHF which was detected by ISH in transgenic embryos as compared to wild type embryos (Fig. 5I-J).

These results suggest that these four genes, *Nkx2-6*, *Raldh2*, *Tbx5* and *Gata4*, are highly sensitive to altered *Tbx1* dosage and some of them may contribute to the SHF-derived defects in the transgenic mice. On the other hand, reduction of expression of *Tbx5* and *Gata4*, whose expression is already at low levels, may not directly cause the OFT defects present in the transgenic mice. However, these findings support our conclusion that most gene expression changes are a result of *Tbx1* dosage alteration and not due to morphological differences. We did not find significant expression changes for the rest of the genes tested in *TBX1* transgenic embryos (data not shown) indicating either that these genes are not dosage-sensitive, or their expression changes were not obvious in some transgenic embryos because the defects caused by increased *Tbx1* dosage were milder than those in the null mutants.

DISCUSSION

Tbx1, the VCFS/DGS gene, is highly expressed in the SHF during embryonic development and *Tbx1*$^{-/-}$ embryos have major OFT defects. In this study, we dissected the caudal pharyngeal region containing the SHF from wild type and *Tbx1*$^{-/-}$ embryos to identify genetic pathways downstream of *Tbx1* required for heart development. We identified a number of critical genes with altered expression in the SHF; most of them have not been previously linked to the SHF or *Tbx1*. What was particularly striking was a downregulation of *Isl1*, *Hod* and *Nkx2-6*, among others, coupled with ectopic expression of genes that promote differentiation, including *Raldh2*, *Gata4*, *Tbx5*, as well as muscle contractile genes in *Tbx1*$^{-/-}$ mutants. In addition, the temporal pattern of expression of these genes indicates that *Tbx1* regulates SHF development no later than E8.75, consistent with results from a study in which *Tbx1* was ablated at different time points in development. It was shown that OFT defects in *Tbx1* mutants occurred at E8.5-

E9.5 (Xu et al., 2005). Recently, *Tbx1* was found to function cell autonomously in the SHF for OFT development (Zhang et al., 2006). Similar gene expression changes were observed when a *Tbx1* conditional allele was inactivated using a pan-mesodermal driver of Cre recombinase, T-Cre. In addition, opposite gene expression changes caused by overexpression of *TBX1*, associated with heart malformations support these findings. Our data for the first time provides a set of genes downstream of *Tbx1* required for the morphogenesis of the cardiac outflow tract.

Tbx1 regulates the balance between myocardial proliferation and differentiation in the SHF through *Isl1*, *Hod* and *Nkx2.6*

Although both FHF and SHF cells are derived from a common pool of mesodermal progenitors in the early embryo, they obtain different cell fates and contribute to distinct regions of the heart during later development (Meilhac et al., 2004). For example, FHF cells start to differentiate into myocardial cells at the cardiac crescent stage, while SHF cells maintain an undifferentiated precursor state until they migrate into the heart (Cai et al., 2003). Therefore, it is important to maintain a proliferating as well as undifferentiated progenitor cell pool in the SHF for appropriate OFT development. Although reduced cell proliferation together with decreased cell contribution to the OFT has been found in *Tbx1*$^{-/-}$ embryos (Xu et al., 2004; Zhang et al., 2006), the molecular mechanisms have remained elusive. Here we found that *Isl1*, *Hod* and *Nkx2.6* are co-expressed with *Tbx1* in the SHF and are downregulated in *Tbx1*$^{-/-}$ embryos. These three genes, particularly the SHF marker, *Isl1*, have key roles in the development of the SHF. Inactivation of *Isl1* results in failed OFT and right ventricle formation as well as reduced posterior atrial development (Cai et al., 2003). It is expressed strongly in SHF precursor cells, required for cell proliferation and is downregulated when cells differentiate into myoblasts (Cai et al., 2003). It has been hypothesized that *Isl1* may act upstream of *Tbx1*, since *Tbx1*$^{-/-}$ mutants have only OFT defects (Kelly, 2005). However, it is not unusual for transcription factors to have important functions at more than one stage of development, regulated by different mechanisms. Our data suggests that *Tbx1* regulates *Isl1* expression levels from E8.5 to E9.0, when the OFT and heart chambers are forming. Based upon the known function of *Isl1* in promoting proliferation and perhaps also suppressing differentiation, we hypothesize that *Tbx1* maintains *Isl1* function in the SHF during OFT development as shown in the model in Figure 6.

In addition to *Isl1*, two other genes, *Hod* and *Nkx2-6*, co-expressed with *Tbx1* in the SHF, were downregulated in *Tbx1*$^{-/-}$ embryos. *Hod* encodes an unusual homeodomain protein that functions at multiple stages in heart development. Some *Hod*$^{-/-}$ embryos have extremely thin ventricular walls (Chen et al., 2002; Shin et al., 2002). In addition to a possible role in promoting proliferation in the SHF, Hod interacts with serum response factor (SRF) to inhibit differentiation by preventing SRF-dependent transcription of muscle structural genes, such as *Actc1*, which was upregulated in *Tbx1*$^{-/-}$ embryos (Chen et al., 2002; Shin et al., 2002). Inactivation of *Tbx1* causes delayed onset of *Hod* expression in the SHF, indicating *Tbx1* may promote cell proliferation and inhibit differentiation through *Hod* (Figure 6). *Hod* is a direct downstream target gene of *Nkx2-5* (Chen et al., 2002; Shin et al., 2002). We found that *Nkx2-5* expression was unaltered in *Tbx1*$^{-/-}$ embryos. This indicates that *Tbx1* regulates *Hod* independent of its regulation by *Nkx2-5*. Of interest, we found another member of *Nk-2* gene family was downregulated in *Tbx1*$^{-/-}$ embryos.

Nkx2-6 belongs to the same *Nk-2* family of homeobox transcription factors as *Nkx2-5*. However, unlike *Nkx2-5* null mutants, which have arrested heart formation at the looping stage (Lyons et al., 1995), homozygous *Nkx2-6* mutant mice are viable and normal (Tanaka et al., 2000). Interestingly, *Nkx2-5/Nkx2-6* double-mutants show some severe pharyngeal and cardiac defects which were not found in any single mutants, indicating a functional overlap between these two genes (Tanaka et al., 2001). In addition, the strong conservation in the homeodomain

between *Nkx2-5* and *Nkx2-6*, as well as expression overlap between them in the SHF also suggests molecular and functional redundancy. Since *Nkx2-5* acts in a genetic pathway upstream of *Hod* (Chen et al., 2002; Shin et al., 2002), and more recently *Nkx2-1*, another *Nk-2* gene was also found to directly regulate *Hod* expression in the lung (Yin et al., 2006), it is possible that *Tbx1* may regulate *Hod* through *Nkx2-6* in the SHF. This hypothesis is also supported by the similar expression dynamics and pattern between *Nkx2-6* and *Hod* in both wild type and $Tbx1^{-/-}$ embryos revealed by qRT-PCR and ISH analysis. The role of *Nkx2-6* in OFT development is further supported by the finding that an *NKX2-6* mutation associates with a family with PTA (Heathcote et al., 2005).

Thus, *Isl1*, *Hod* and *Nkx2-6* are important genes for the normal development of the OFT, but besides *Isl1*, they did not have defined roles in the SHF, especially downstream of *Tbx1*. Our data suggests that *Tbx1* supports expression of these genes to maintain the balance between proliferation and differentiation of progenitor cells in the SHF (Fig. 6).

Tbx1 prevents premature differentiation in the SHF through the *Raldh2* genetic pathway

Raldh2, *Tbx5* and *Gata4* play essential roles in regulating myocardial differentiation and patterning of the linear heart tube. In particular, *Raldh2* is expressed in the posterior mesoderm precursors of the inflow part of the heart tube (Moss et al., 1998). Localized synthesis of retinoic acid (RA) by *Raldh2* determines atrial cell fates, whereas ventricular cell fates occur in the absence of *Raldh2* expression and RA signaling (reviewed by Xavier-Neto et al., 2001). Inhibition of endogenous RA synthesis represses expression of atrial-specific markers and results in an oversized ventricle and aplastic atria. Conversely, exogenous RA induces atrial-specific gene expression and produces a heart with hyperplastic atria but missing ventricles and OFT (Chazaud et al., 1999; Hochgreb et al., 2003; Xavier-Neto et al., 1999; Yutzey et al., 1994).

The two genes, *Tbx5* and *Gata4*, physically interact to regulate transcription of downstream genes (Garg et al., 2003). Both are expressed in a posterior-to-anterior gradient in the linear heart tube during heart development (Bruneau et al., 1999; Molkentin et al., 1997) and both act downstream of *Raldh2* (Kostetskii et al., 1999; Liberatore et al., 2000; Niederreither et al., 2001). In vitro experiments showed that *Gata4* is necessary and sufficient to induce cardiac differentiation marked by a number of myocardial structural genes including several genes found in this study, *Actc1*, *Myh6*, *Myl4*, and *Tnnc1* (Grepin et al., 1997; Grepin et al., 1995; Ip et al., 1994; Jiang and Evans, 1996; Molkentin et al., 1994; Sepulveda et al., 1998; Zeisberg et al., 2005). Similarly, *Tbx5* overexpression in cell lines can also accelerate myocardial differentiation and induce *Myh6* expression (Ching et al., 2005; Hiroi et al., 2001). The role of *Tbx5* in anterior-posterior (AP) patterning of the heart is further suggested via mouse models. $Tbx5^{-/-}$ mouse embryos have hypoplastic posterior heart structures including the left ventricle, atria, and inflow tract (Bruneau et al., 2001). Furthermore, ectopic overexpression of *Tbx5* in both chick and mice results in loss of ventricular-specific gene expression and retardation of ventricular chamber morphogenesis (Liberatore et al., 2000; Takeuchi et al., 2003). Our data is consistent with *Tbx1* acting to restrict myocardial differentiation in the SHF through a *Raldh2-Tbx5/Gata4-Myh6/Myl7/Actc1* pathway, which are all ectopically expressed in the SHF of $Tbx1^{-/-}$ embryos (Fig. 6).

Gene expression changes versus altered morphology

The caudal pharyngeal apparatus fails to develop in $Tbx1^{-/-}$ embryos due to defects in neural crest migration (Moraes et al., 2005; Vitelli et al., 2002a). Seemingly, gene expression changes we found in $Tbx1^{-/-}$ embryos could be caused by morphological defects in these embryos. There are several reasons why we believe that it is not the case. The first and most important is that $Tbx1^{-/-}$ embryos at E8.75 did not yet have grossly detectable morphological defects though

subtle changes in cell populations might have occurred. Second, if changes in gene expression were due to morphological defects in the caudal pharyngeal region of *Tbx1*$^{-/-}$ embryos, we would expect to see a more general profile of genes with expression changes. However, according to our experimental results, the expression levels and patterns of many other SHF and myocardial marker genes such as *Nkx2-5*, *Foxh1*, *Mef2c*, and *Hand1* (see Table S6 in the supplementary material) were not changed in *Tbx1*$^{-/-}$ embryos, indicating very selective and specific effect. Third, *Tbx1* is co-expressed with these genes in the SHF, indicating a possible role of Tbx1 in directly regulating transcription of a subset of these genes. Finally, we found the opposite expression changes for some of the same genes in BAC transgenic mice overexpressing *TBX1*, in the absence of morphological defects in the caudal pharyngeal apparatus. Thus, we believe that most of the changes observed at E8.75 and perhaps an important subset later, resulted from gene expression changes in the SHF cells and not due to gross alterations in cell populations.

We also noted some inconsistencies between our microarray data and a few previous reports about expression changes of Tbx1-regulated genes. For example, we previously showed that *Pitx2* expression was downregulated while *Isl1* expression did not change in the SHF of E8.0 *Tbx1* -/- embryos (Nowotschin et al., 2006). Our microarray analysis found an increased level of *Pitx2* expression at E9.75 (Table S2) which was not confirmed by qRT-PCR (data not shown). Decreased *Isl1* expression at E8.75 (Table 1), might suggest different responses to Tbx1-regulation at different developmental stages. Another example is expression of *Foxa2* and *Fgf8*, which was previously reported to be downregulated in the SHF of *Tbx1* mutant embryos (Hu et al., 2004). Although none of them was found by our microarray experiments, qRT-PCR experiments for these two genes showed significant downregulation as previously reported (data not shown). This is why we validated all gene changes of interest by qRT-PCR and ISH studies.

Conclusions

In the model shown in Figure 6, we hypothesize that *Tbx1* maintains the balance between the proliferation and differentiation of myocardial progenitor cells in the SHF by activating, either directly or indirectly, *Isl1*, *Hod* and *Nkx2-6*. A *Raldh2-Tbx5/Gata4* genetic pathway, normally repressed by *Tbx1*, may also contribute to the role of *Tbx1* in preventing premature differentiation of the SHF cells. Inactivation of *Tbx1* in the pharyngeal mesoderm causes the abnormal expression of these genes, which further disrupts the appropriate proliferation-versus-differentiation balance required for normal contribution of SHF cells to the OFT myocardium, resulting in OFT defects. If the changes are cell autonomous, it is possible that some could be direct downstream transcriptional target genes of Tbx1. For example, *Isl1*, *Gata4*, and *Tbx5* contain one or multiple T-box consensus binding sites in their promoter or enhancer regions (Cai et al., 2005;Heicklen-Klein and Evans, 2004;Sun et al., 2004). We also examined the DNA sequence surrounding the first exon of *Raldh2* and found a conserved T-box consensus sequence present (see Fig. S4 in the supplementary material), suggesting that Tbx1 might be able to regulate *Raldh2* expression levels directly.

Interestingly, for most of these genes, their expression changes more specifically occurred in the caudal/posterior part of the SHF region, which may be caused by stronger expression of *Tbx1* itself in the caudal pharyngeal region (Fig. 2B). Another interpretation is that *Tbx1* may play a role in regulating AP patterning of the SHF since some of these genes we found such as *Raldh2*, *Tbx5*, and *Gata4* have well-known functions in regulating AP patterning of the heart tube, as we discussed above. Further detailed analysis will be necessary to address this question. In addition, characterization of additional genes found by microarray analysis would likely expand the genetic network described here. Finally, nucleotide variations in some of these genes might influence the expressivity of VCFS/DGS, thereby serving as genetic modifiers.

Supplementary Material

Refer to Web version on PubMed Central for supplementary material.

Acknowledgements

We thank Dr Radma Mahmood, Dr Xin Zheng, Mr David Reynolds, Mr Wen Tran, and Ms Shaoqing Yu for technical assistance; Dr. Mark Lewandoski for *T-Cre* transgenic mouse strain; Dr Marina Campione for ISH probes. We also thank Dr Jonathan Epstein, Dr Arthur Skoultchi, and Mr Evan Braunstein for critical reading and helpful comments on the manuscript. This work was supported by grants from NIDCD (R01DC05186-03) and the March of Dimes (FY2005-443) (B.E.M.).

References

Aggarwal VS, Liao J, Bondarev A, Schimmang T, Lewandoski M, Locker J, Shanske A, Campione M, Morrow BE. Dissection of Tbx1 and Fgf interactions in mouse models of 22q11DS suggests functional redundancy. Hum Mol Genet 2006;15:3219–28. [PubMed: 17000704]

Arnold JS, Werling U, Braunstein EM, Liao J, Nowotschin S, Edelmann W, Hebert JM, Morrow BE. Inactivation of Tbx1 in the pharyngeal endoderm results in 22q11DS malformations. Development 2006;133:977–87. [PubMed: 16452092]

Biben C, Hatzistavrou T, Harvey RP. Expression of NK-2 class homeobox gene Nkx2-6 in foregut endoderm and heart. Mech Dev 1998;73:125–7. [PubMed: 9545560]

Bruneau BG. Transcriptional regulation of vertebrate cardiac morphogenesis. Circ Res 2002;90:509–19. [PubMed: 11909814]

Bruneau BG, Logan M, Davis N, Levi T, Tabin CJ, Seidman JG, Seidman CE. Chamber-specific cardiac expression of Tbx5 and heart defects in Holt-Oram syndrome. Dev Biol 1999;211:100–8. [PubMed: 10373308]

Bruneau BG, Nemer G, Schmitt JP, Charron F, Robitaille L, Caron S, Conner DA, Gessler M, Nemer M, Seidman CE, Seidman JG. A murine model of Holt-Oram syndrome defines roles of the T-box transcription factor Tbx5 in cardiogenesis and disease. Cell 2001;106:709–21. [PubMed: 11572777]

Buckingham M, Meilhac S, Zaffran S. Building the mammalian heart from two sources of myocardial cells. Nat Rev Genet 2005;6:826–35. [PubMed: 16304598]

Cai CL, Liang X, Shi Y, Chu PH, Pfaff SL, Chen J, Evans S. Isl1 identifies a cardiac progenitor population that proliferates prior to differentiation and contributes a majority of cells to the heart. Dev Cell 2003;5:877–89. [PubMed: 14667410]

Cai CL, Zhou W, Yang L, Bu L, Qyang Y, Zhang X, Li X, Rosenfeld MG, Chen J, Evans S. T-box genes coordinate regional rates of proliferation and regional specification during cardiogenesis. Development 2005;132:2475–87. [PubMed: 15843407]

Chapman DL, Garvey N, Hancock S, Alexiou M, Agulnik SI, Gibson-Brown JJ, Cebra-Thomas J, Bollag RJ, Silver LM, Papaioannou VE. Expression of the T-box family genes, Tbx1-Tbx5, during early mouse development. Dev Dyn 1996;206:379–90. [PubMed: 8853987]

Chazaud C, Chambon P, Dolle P. Retinoic acid is required in the mouse embryo for left-right asymmetry determination and heart morphogenesis. Development 1999;126:2589–96. [PubMed: 10331971]

Chen F, Kook H, Milewski R, Gitler AD, Lu MM, Li J, Nazarian R, Schnepp R, Jen K, Biben C, Runke G, Mackay JP, Novotny J, Schwartz RJ, Harvey RP, Mullins MC, Epstein JA. Hop is an unusual homeobox gene that modulates cardiac development. Cell 2002;110:713–23. [PubMed: 12297045]

Ching YH, Ghosh TK, Cross SJ, Packham EA, Honeyman L, Loughna S, Robinson TE, Dearlove AM, Ribas G, Bonser AJ, Thomas NR, Scotter AJ, Caves LS, Tyrrell GP, Newbury-Ecob RA, Munnich A, Bonnet D, Brook JD. Mutation in myosin heavy chain 6 causes atrial septal defect. Nat Genet 2005;37:423–8. [PubMed: 15735645]

DiGeorge A. A new concept of the cellular basis of immunity. J Pediatr 1965;67:907.

Franco D, Lamers WH, Moorman AF. Patterns of expression in the developing myocardium: towards a morphologically integrated transcriptional model. Cardiovasc Res 1998;38:25–53. [PubMed: 9683906]

Funke B, Epstein JA, Kochilas LK, Lu MM, Pandita RK, Liao J, Bauerndistel R, Schuler T, Schorle H, Brown MC, Adams J, Morrow BE. Mice overexpressing genes from the 22q11 region deleted in

velo-cardio-facial syndrome/DiGeorge syndrome have middle and inner ear defects. Hum Mol Genet 2001;10:2549–56. [PubMed: 11709542]

Garg V, Kathiriya IS, Barnes R, Schluterman MK, King IN, Butler CA, Rothrock CR, Eapen RS, Hirayama-Yamada K, Joo K, Matsuoka R, Cohen JC, Srivastava D. GATA4 mutations cause human congenital heart defects and reveal an interaction with TBX5. Nature 2003;424:443–7. [PubMed: 12845333]

Grepin C, Nemer G, Nemer M. Enhanced cardiogenesis in embryonic stem cells overexpressing the GATA-4 transcription factor. Development 1997;124:2387–95. [PubMed: 9199365]

Grepin C, Robitaille L, Antakly T, Nemer M. Inhibition of transcription factor GATA-4 expression blocks in vitro cardiac muscle differentiation. Mol Cell Biol 1995;15:4095–102. [PubMed: 7623805]

Guris DL, Duester G, Papaioannou VE, Imamoto A. Dose-dependent interaction of Tbx1 and Crkl and locally aberrant RA signaling in a model of del22q11 syndrome. Dev Cell 2006;10:81–92. [PubMed: 16399080]

Heathcote K, Braybrook C, Abushaban L, Guy M, Khetyar ME, Patton MA, Carter ND, Scambler PJ, Syrris P. Common arterial trunk associated with a homeodomain mutation of NKX2.6. Hum Mol Genet 2005;14:585–93. [PubMed: 15649947]

Heicklen-Klein A, Evans T. T-box binding sites are required for activity of a cardiac GATA-4 enhancer. Dev Biol 2004;267:490–504. [PubMed: 15013808]

Hiroi Y, Kudoh S, Monzen K, Ikeda Y, Yazaki Y, Nagai R, Komuro I. Tbx5 associates with Nkx2-5 and synergistically promotes cardiomyocyte differentiation. Nat Genet 2001;28:276–80. [PubMed: 11431700]

Hochgreb T, Linhares VL, Menezes DC, Sampaio AC, Yan CY, Cardoso WV, Rosenthal N, Xavier-Neto J. A caudorostral wave of RALDH2 conveys anteroposterior information to the cardiac field. Development 2003;130:5363–74. [PubMed: 13129847]

Hu T, Yamagishi H, Maeda J, McAnally J, Yamagishi C, Srivastava D. Tbx1 regulates fibroblast growth factors in the anterior heart field through a reinforcing autoregulatory loop involving forkhead transcription factors. Development 2004;131:5491–502. [PubMed: 15469978]

Ip HS, Wilson DB, Heikinheimo M, Tang Z, Ting CN, Simon MC, Leiden JM, Parmacek MS. The GATA-4 transcription factor transactivates the cardiac muscle-specific troponin C promoter-enhancer in nonmuscle cells. Mol Cell Biol 1994;14:7517–26. [PubMed: 7935467]

Ivins S, Lammerts van Beuren K, Roberts C, James C, Lindsay E, Baldini A, Ataliotis P, Scambler PJ. Microarray analysis detects differentially expressed genes in the pharyngeal region of mice lacking Tbx1. Dev Biol 2005;285:554–69. [PubMed: 16109395]

Jerome LA, Papaioannou VE. DiGeorge syndrome phenotype in mice mutant for the T-box gene, Tbx1. Nat Genet 2001;27:286–91. [PubMed: 11242110]

Jiang Y, Evans T. The Xenopus GATA-4/5/6 genes are associated with cardiac specification and can regulate cardiac-specific transcription during embryogenesis. Dev Biol 1996;174:258–70. [PubMed: 8631498]

Kelly RG. Molecular inroads into the anterior heart field. Trends Cardiovasc Med 2005;15:51–6. [PubMed: 15885570]

Kelly RG, Buckingham ME. The anterior heart-forming field: voyage to the arterial pole of the heart. Trends Genet 2002;18:210–6. [PubMed: 11932022]

Kostetskii I, Jiang Y, Kostetskaia E, Yuan S, Evans T, Zile M. Retinoid signaling required for normal heart development regulates GATA-4 in a pathway distinct from cardiomyocyte differentiation. Dev Biol 1999;206:206–18. [PubMed: 9986733]

Liao J, Kochilas L, Nowotschin S, Arnold JS, Aggarwal VS, Epstein JA, Brown MC, Adams J, Morrow BE. Full spectrum of malformations in velo-cardio-facial syndrome/DiGeorge syndrome mouse models by altering Tbx1 dosage. Hum Mol Genet 2004;13:1577–85. [PubMed: 15190012]

Liberatore CM, Searcy-Schrick RD, Yutzey KE. Ventricular expression of tbx5 inhibits normal heart chamber development. Dev Biol 2000;223:169–80. [PubMed: 10864469]

Lindsay EA, Vitelli F, Su H, Morishima M, Huynh T, Pramparo T, Jurecic V, Ogunrinu G, Sutherland HF, Scambler PJ, Bradley A, Baldini A. Tbx1 haploinsufficieny in the DiGeorge syndrome region causes aortic arch defects in mice. Nature 2001;410:97–101. [PubMed: 11242049]

Lyons I, Parsons LM, Hartley L, Li R, Andrews JE, Robb L, Harvey RP. Myogenic and morphogenetic defects in the heart tubes of murine embryos lacking the homeo box gene Nkx2-5. Genes Dev 1995;9:1654–66. [PubMed: 7628699]

Marguerie A, Bajolle F, Zaffran S, Brown NA, Dickson C, Buckingham ME, Kelly RG. Congenital heart defects in Fgfr2-IIIb and Fgf10 mutant mice. Cardiovasc Res 2006;71:50–60. [PubMed: 16687131]

Meilhac SM, Esner M, Kelly RG, Nicolas JF, Buckingham ME. The clonal origin of myocardial cells in different regions of the embryonic mouse heart. Dev Cell 2004;6:685–98. [PubMed: 15130493]

Merscher S, Funke B, Epstein JA, Heyer J, Puech A, Lu MM, Xavier RJ, Demay MB, Russell RG, Factor S, Tokooya K, Jore BS, Lopez M, Pandita RK, Lia M, Carrion D, Xu H, Schorle H, Kobler JB, Scambler P, Wynshaw-Boris A, Skoultchi AI, Morrow BE, Kucherlapati R. TBX1 is responsible for cardiovascular defects in velo-cardio-facial/DiGeorge syndrome. Cell 2001;104:619–29. [PubMed: 11239417]

Molkentin JD, Kalvakolanu DV, Markham BE. Transcription factor GATA-4 regulates cardiac muscle-specific expression of the alpha-myosin heavy-chain gene. Mol Cell Biol 1994;14:4947–57. [PubMed: 8007990]

Molkentin JD, Lin Q, Duncan SA, Olson EN. Requirement of the transcription factor GATA4 for heart tube formation and ventral morphogenesis. Genes Dev 1997;11:1061–72. [PubMed: 9136933]

Moraes F, Novoa A, Jerome-Majewska LA, Papaioannou VE, Mallo M. Tbx1 is required for proper neural crest migration and to stabilize spatial patterns during middle and inner ear development. Mech Dev 2005;122:199–212. [PubMed: 15652707]

Morrow B, Goldberg R, Carlson C, Das Gupta R, Sirotkin H, Collins J, Dunham I, O'Donnell H, Scambler P, Shprintzen R, et al. Molecular definition of the 22q11 deletions in velo-cardio-facial syndrome. Am J Hum Genet 1995;56:1391–403. [PubMed: 7762562]

Moss JB, Xavier-Neto J, Shapiro MD, Nayeem SM, McCaffery P, Drager UC, Rosenthal N. Dynamic patterns of retinoic acid synthesis and response in the developing mammalian heart. Dev Biol 1998;199:55–71. [PubMed: 9676192]

Niederreither K, Vermot J, Messaddeq N, Schuhbaur B, Chambon P, Dolle P. Embryonic retinoic acid synthesis is essential for heart morphogenesis in the mouse. Development 2001;128:1019–31. [PubMed: 11245568]

Nikolova M, Chen X, Lufkin T. Nkx2.6 expression is transiently and specifically restricted to the branchial region of pharyngeal-stage mouse embryos. Mech Dev 1997;69:215–8. [PubMed: 9486544]

Nowotschin S, Liao J, Gage PJ, Epstein JA, Campione M, Morrow BE. Tbx1 affects asymmetric cardiac morphogenesis by regulating Pitx2 in the secondary heart field. Development 2006;133:1565–73. [PubMed: 16556915]

Paylor R, Glaser B, Mupo A, Ataliotis P, Spencer C, Sobotka A, Sparks C, Choi CH, Oghalai J, Curran S, Murphy KC, Monks S, Williams N, O'Donovan MC, Owen MJ, Scambler PJ, Lindsay E. Tbx1 haploinsufficiency is linked to behavioral disorders in mice and humans: implications for 22q11 deletion syndrome. Proc Natl Acad Sci U S A 2006;103:7729–34. [PubMed: 16684884]

Perantoni AO, Timofeeva O, Naillat F, Richman C, Pajni-Underwood S, Wilson C, Vainio S, Dove LF, Lewandoski M. Inactivation of FGF8 in early mesoderm reveals an essential role in kidney development. Development 2005;132:3859–71. [PubMed: 16049111]

Pikkarainen S, Tokola H, Kerkela R, Ruskoaho H. GATA transcription factors in the developing and adult heart. Cardiovasc Res 2004;63:196–207. [PubMed: 15249177]

Sepulveda JL, Belaguli N, Nigam V, Chen CY, Nemer M, Schwartz RJ. GATA-4 and Nkx-2.5 coactivate Nkx-2 DNA binding targets: role for regulating early cardiac gene expression. Mol Cell Biol 1998;18:3405–15. [PubMed: 9584181]

Shaikh TH, Kurahashi H, Saitta SC, O'Hare AM, Hu P, Roe BA, Driscoll DA, McDonald-McGinn DM, Zackai EH, Budarf ML, Emanuel BS. Chromosome 22-specific low copy repeats and the 22q11.2 deletion syndrome: genomic organization and deletion endpoint analysis. Hum Mol Genet 2000;9:489–501. [PubMed: 10699172]

Shin CH, Liu ZP, Passier R, Zhang CL, Wang DZ, Harris TM, Yamagishi H, Richardson JA, Childs G, Olson EN. Modulation of cardiac growth and development by HOP, an unusual homeodomain protein. Cell 2002;110:725–35. [PubMed: 12297046]

Shprintzen RJ, Goldberg RB, Lewin ML, Sidoti EJ, Berkman MD, Argamaso RV, Young D. A new syndrome involving cleft palate, cardiac anomalies, typical facies, and learning disabilities: velo-cardio-facial syndrome. Cleft Palate J 1978;15:56–62. [PubMed: 272242]

Soriano P. Generalized lacZ expression with the ROSA26 Cre reporter strain. Nat Genet 1999;21:70–1. [PubMed: 9916792]

Stoller JZ, Epstein JA. Identification of a novel nuclear localization signal in Tbx1 that is deleted in DiGeorge syndrome patients harboring the 1223delC mutation. Hum Mol Genet 2005;14:885–92. [PubMed: 15703190]

Sun G, Lewis LE, Huang X, Nguyen Q, Price C, Huang T. TBX5, a gene mutated in Holt-Oram syndrome, is regulated through a GC box and T-box binding elements (TBEs). J Cell Biochem 2004;92:189–99. [PubMed: 15095414]

Takeuchi JK, Ohgi M, Koshiba-Takeuchi K, Shiratori H, Sakaki I, Ogura K, Saijoh Y, Ogura T. Tbx5 specifies the left/right ventricles and ventricular septum position during cardiogenesis. Development 2003;130:5953–64. [PubMed: 14573514]

Tanaka M, Schinke M, Liao HS, Yamasaki N, Izumo S. Nkx2.5 and Nkx2.6, homologs of Drosophila tinman, are required for development of the pharynx. Mol Cell Biol 2001;21:4391–8. [PubMed: 11390666]

Tanaka M, Yamasaki N, Izumo S. Phenotypic characterization of the murine Nkx2.6 homeobox gene by gene targeting. Mol Cell Biol 2000;20:2874–9. [PubMed: 10733590]

Verzi MP, McCulley DJ, De Val S, Dodou E, Black BL. The right ventricle, outflow tract, and ventricular septum comprise a restricted expression domain within the secondary/anterior heart field. Dev Biol 2005;287:134–45. [PubMed: 16188249]

Vitelli F, Morishima M, Taddei I, Lindsay EA, Baldini A. Tbx1 mutation causes multiple cardiovascular defects and disrupts neural crest and cranial nerve migratory pathways. Hum Mol Genet 2002a; 11:915–22. [PubMed: 11971873]

Vitelli F, Taddei I, Morishima M, Meyers EN, Lindsay EA, Baldini A. A genetic link between Tbx1 and fibroblast growth factor signaling. Development 2002b;129:4605–11. [PubMed: 12223416]

Xavier-Neto J, Neville CM, Shapiro MD, Houghton L, Wang GF, Nikovits W Jr, Stockdale FE, Rosenthal N. A retinoic acid-inducible transgenic marker of sino-atrial development in the mouse heart. Development 1999;126:2677–87. [PubMed: 10331979]

Xavier-Neto J, Rosenthal N, Silva FA, Matos TG, Hochgreb T, Linhares VL. Retinoid signaling and cardiac anteroposterior segmentation. Genesis 2001;31:97–104. [PubMed: 11747199]

Xu H, Cerrato F, Baldini A. Timed mutation and cell-fate mapping reveal reiterated roles of Tbx1 during embryogenesis, and a crucial function during segmentation of the pharyngeal system via regulation of endoderm expansion. Development 2005;132:4387–95. [PubMed: 16141220]

Xu H, Morishima M, Wylie JN, Schwartz RJ, Bruneau BG, Lindsay EA, Baldini A. Tbx1 has a dual role in the morphogenesis of the cardiac outflow tract. Development 2004;131:3217–27. [PubMed: 15175244]

Yagi H, Furutani Y, Hamada H, Sasaki T, Asakawa S, Minoshima S, Ichida F, Joo K, Kimura M, Imamura S, Kamatani N, Momma K, Takao A, Nakazawa M, Shimizu N, Matsuoka R. Role of TBX1 in human del22q11.2 syndrome. Lancet 2003;362:1366–73. [PubMed: 14585638]

Yin Z, Gonzales L, Kolla V, Rath N, Zhang Y, Lu MM, Kimura S, Ballard PL, Beers MF, Epstein JA, Morrisey EE. Hop functions downstream of Nkx2.1 and GATA6 to mediate HDAC-dependent negative regulation of pulmonary gene expression. Am J Physiol Lung Cell Mol Physiol 2006;291:L191–9. [PubMed: 16510470]

Yutzey KE, Rhee JT, Bader D. Expression of the atrial-specific myosin heavy chain AMHC1 and the establishment of anteroposterior polarity in the developing chicken heart. Development 1994;120:871–83. [PubMed: 7600964]

Zeisberg EM, Ma Q, Juraszek AL, Moses K, Schwartz RJ, Izumo S, Pu WT. Morphogenesis of the right ventricle requires myocardial expression of Gata4. J Clin Invest 2005;115:1522–31. [PubMed: 15902305]

Zhang Z, Huynh T, Baldini A. Mesodermal expression of Tbx1 is necessary and sufficient for pharyngeal arch and cardiac outflow tract development. Development 2006;133:3587–95. [PubMed: 16914493]

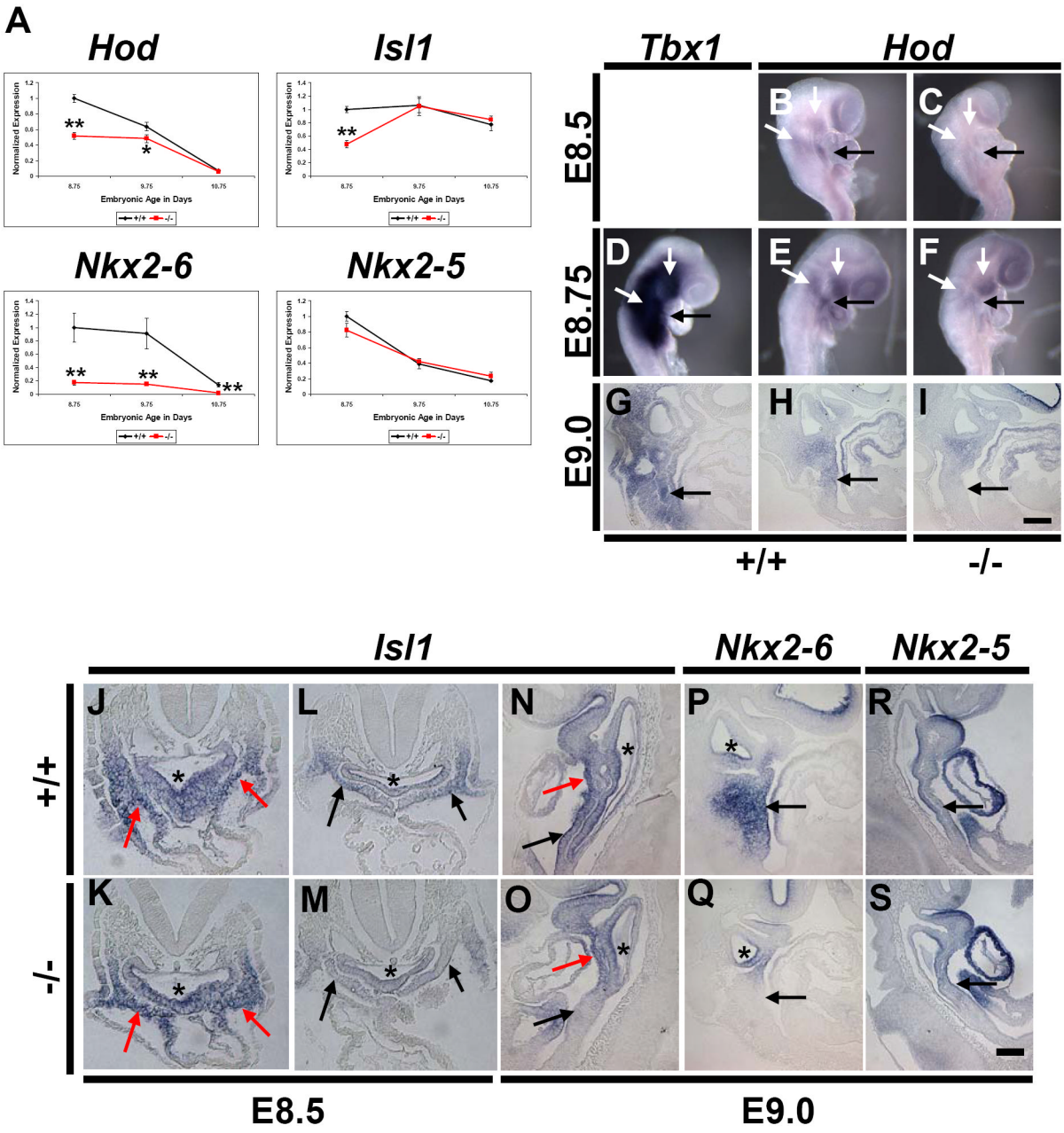

Fig. 1. Validation of altered expression for selected downregulated genes in the SHF of *Tbx1*$^{-/-}$ embryos by qRT-PCR and ISH

(A) Developmental time courses of the expression of *Hod*, *Isl1*, *Nkx2-6*, and *Nkx2-5*, which were generated from qRT-PCR data. For these and all time-course graphs in other figures: values are means of at least three samples and normalized by expression levels of wild type samples at E8.75. **p*-value <0.05, ***p*-value<0.01 (calculated by two-tailed unpaired Student's *t*-test). Error bars represent standard deviation. Note the significant decreased expression of *Hod*, *Isl1*, *Nkx2-6* in *Tbx1*$^{-/-}$ embryos at E8.75, while *Nkx2-5* expression is not changed.

(B-I) Reduced *Hod* expression in the pharyngeal core mesoderm (white arrow) and SHF (black arrow) of *Tbx1*$^{-/-}$ embryos (C,F,I) compared with wild type embryos (B,E,H) and its overlap with the *Tbx1* expression domain in these regions of wild type embryos (D,G) at E8.5 (B,C),

E8.75 (D-F), and E9.0 (G-I). B-F depict whole mount ISH analysis and G-I show sagittal sections cut from whole mount ISH stained embryos.

(J-O) Reduced *Isl1* expression in the caudal part (black arrow) but not the cranial part (red arrow) of the SHF in *Tbx1*$^{-/-}$ embryos (K,M,O) compared with wild type embryos (J,L,N) at E8.5 (J-M) and E9.0 (N,O). J-M are transverse sections and N, O are sagittal sections. *Isl1* expression in the pharyngeal pouch endoderm (asterisk) also remains intact.

(P-S)*Nkx2-6* expression in is absent in the caudal part of the SHF (arrow), while its expression in the pharyngeal pouch endoderm (asterisk) is still present in *Tbx1*$^{-/-}$ embryos (Q) compared with wild type embryos (P) at E9.0. In contrast, *Nkx2-5* expression has no difference in wild type (R) and *Tbx1*$^{-/-}$ (S) embryos. All sections are sagittal.

Scale bars: 300 μm in B-I; 200 μm in J-S.

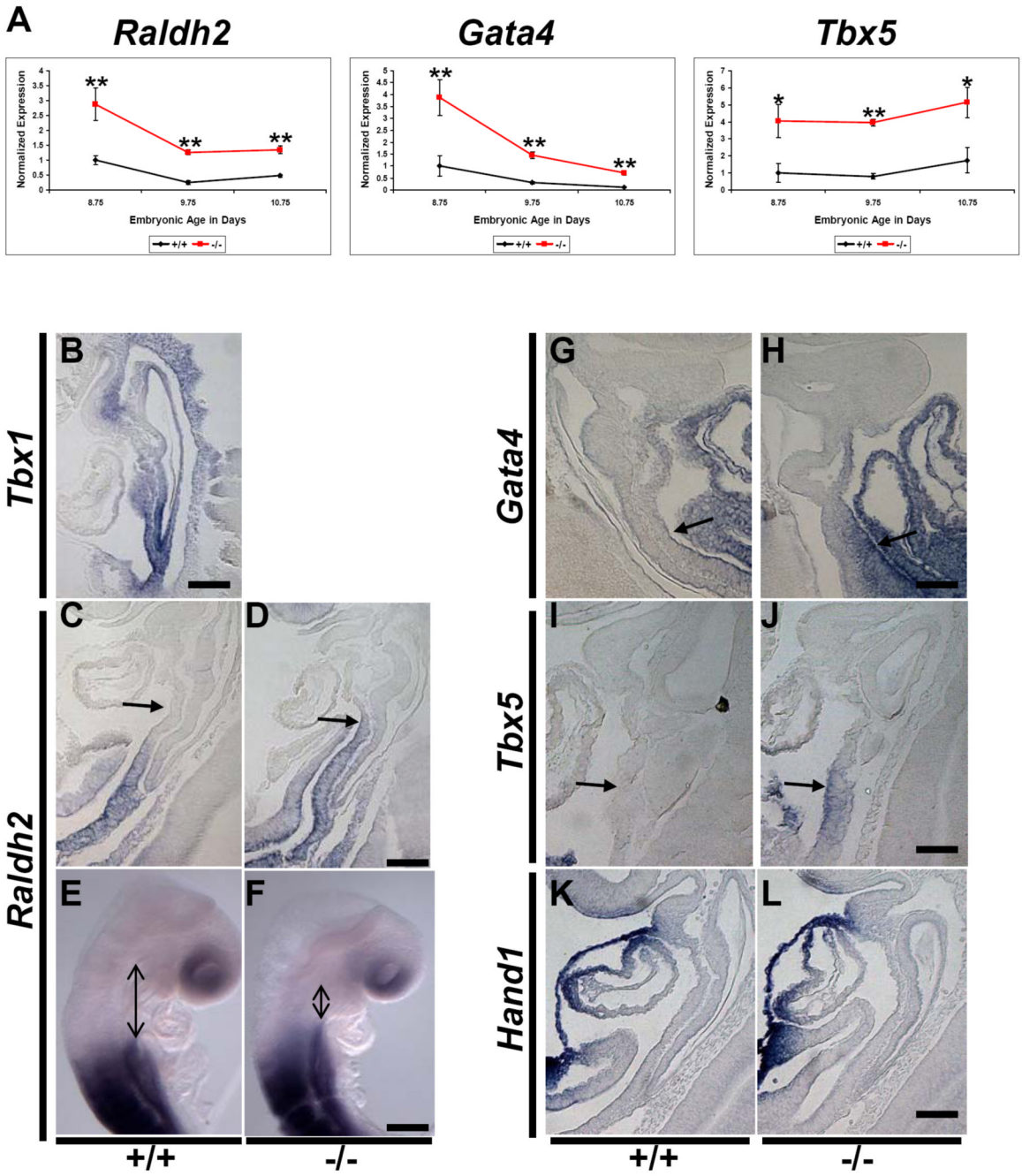

Fig. 2. Validation of altered expression for selected upregulated genes in the SHF of *Tbx1*$^{-/-}$ embryos by qRT-PCR and ISH

(A) Developmental time courses of the expression of *Raldh2*, *Gata4*, and *Tbx5*, which were generated from qRT-PCR data. Note the significant increased expression of these three genes in *Tbx1*$^{-/-}$ embryos at all three stages.

(B-F) Sagittal sectioned (C,D) or whole mount ISH (E,F) at E9.0 show expanded expression (arrow) of *Raldh2* in the SHF of *Tbx1*$^{-/-}$ embryos (D,F) compared with wild type embryos (C,E), which also overlap *Tbx1* expression domain in the SHF of wild type embryos (B). Double-headed arrows in E and F indicate the relative distance between the cranial border of *Raldh2* expression and the caudal border of the first arch.

(G-L) Sagittal sections from E9.0 whole mount ISH stained embryos show expression (arrow) of *Gata4* (G,H), *Tbx5* (I,J) and *Hand1* (K,L) in the SHF of *Tbx1*$^{-/-}$ embryos (H,J,L) compared with wild type embryos (G,I,K). Note the ectopic expression of *Gata4* and *Tbx5* but not *Hand1* in *Tbx1*$^{-/-}$ embryos.
Scale bars: 200 μm in B-F and K-L; 150 μm in G-J

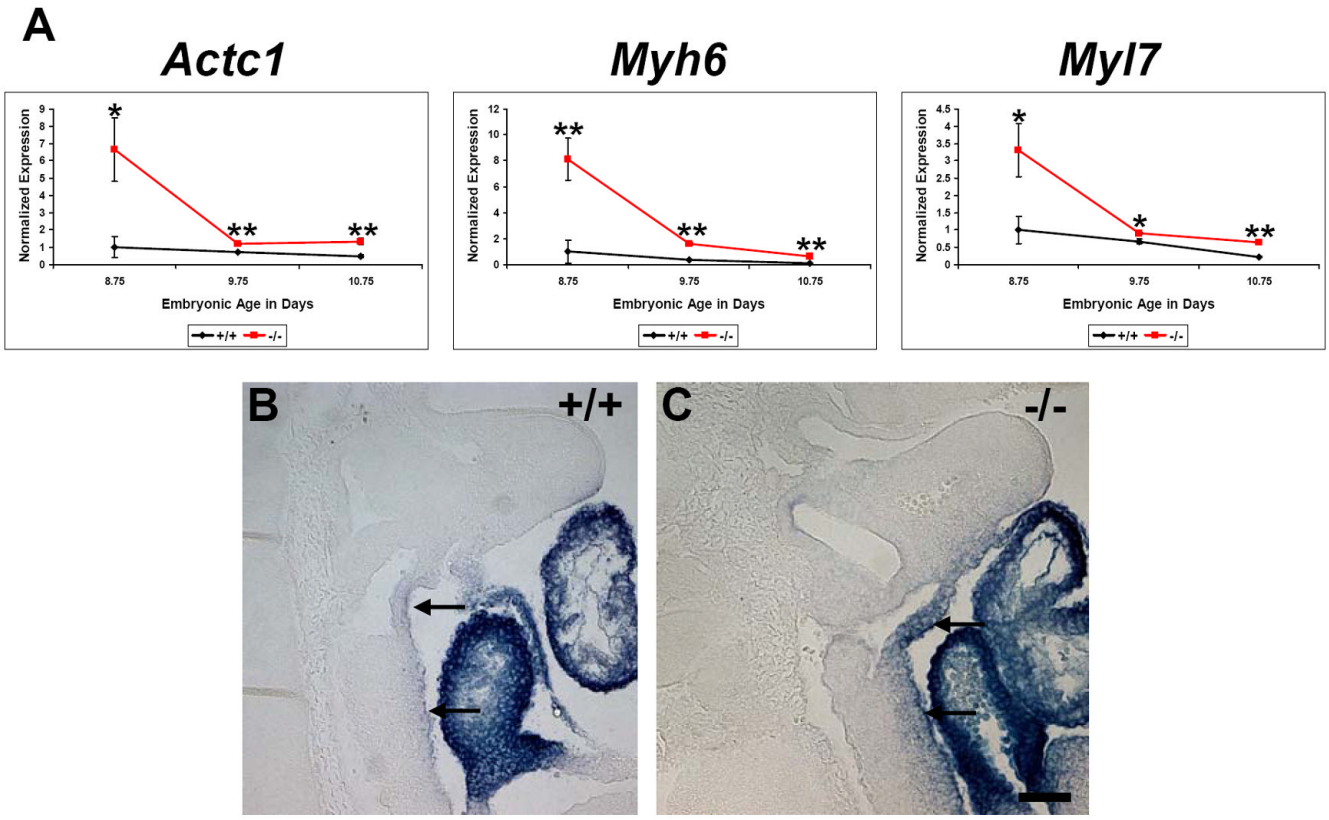

Fig. 3. Validation of altered expression for selected muscle structural genes in the SHF of *Tbx1*$^{-/-}$ embryos by qRT-PCR and ISH

(A) Developmental time courses of the expression of muscle structural genes *Actc1*, *Myh6*, and *Myl7*, which were generated from qRT-PCR data. Note the significant increased expression of these genes in *Tbx1*$^{-/-}$ embryos at all three stages.

(B-C) Sagittal sections from E9.0 whole mount ISH stained embryos show increased expression of *Myh6* (arrow) in the SHF of *Tbx1*$^{-/-}$ embryos (C) compared with wild type embryos (B).

Scale bars: 150 μm.

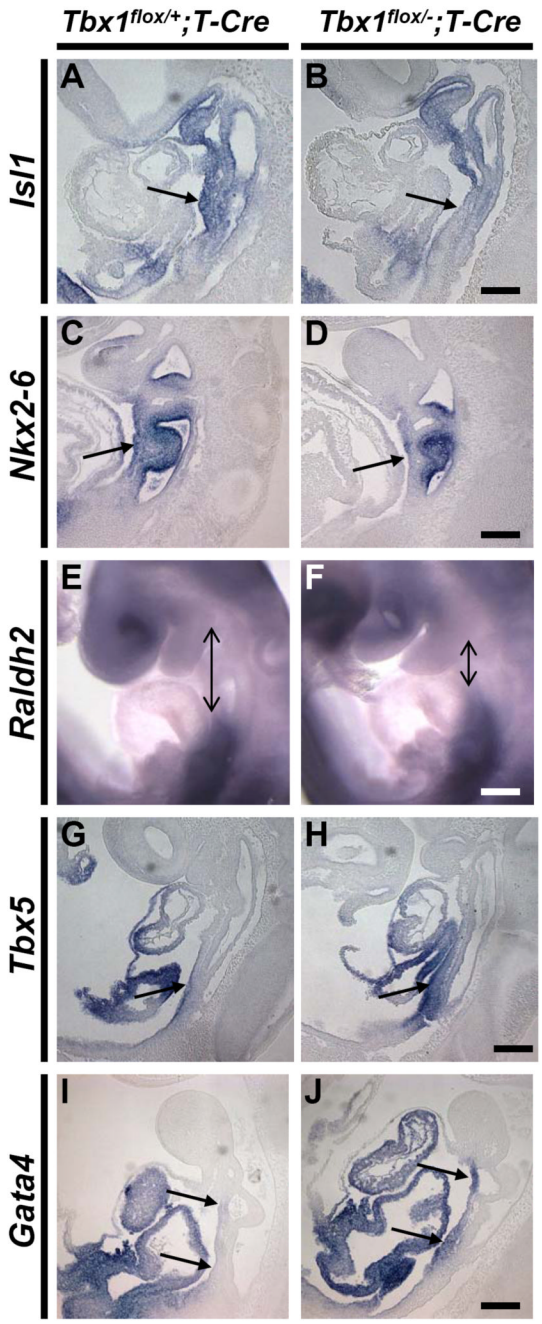

Fig. 4. Partial inactivation of *Tbx1* in mesoderm causes the same gene expression changes as those in *Tbx1*$^{-/-}$ embryos

Sagittal sectioned (A-D,G-J) or whole mount (E,F) ISH at E9.0 (A,B,E-H) or E9.5 (C,D,I,J) show the same expression changes (arrow) in *Tbx1*$^{flox/-}$*;T-Cre* embryos (B,D,F,H,J) compared with *Tbx1*$^{flox/+}$*;T-Cre* embryos (A,C,E,G,I) for *Isl1* (A,B), *Nkx2-6* (C,D), *Raldh2* (E,F), *Tbx5* (G,H), and *Gata4* (I,J). Double-headed arrows indicate the relative distance between the cranial border of *Raldh2* expression and the caudal border of the first arch.
Scale bars: 200 μm in A,B,E,F,G,H; 400 μm in C,D,I,J.

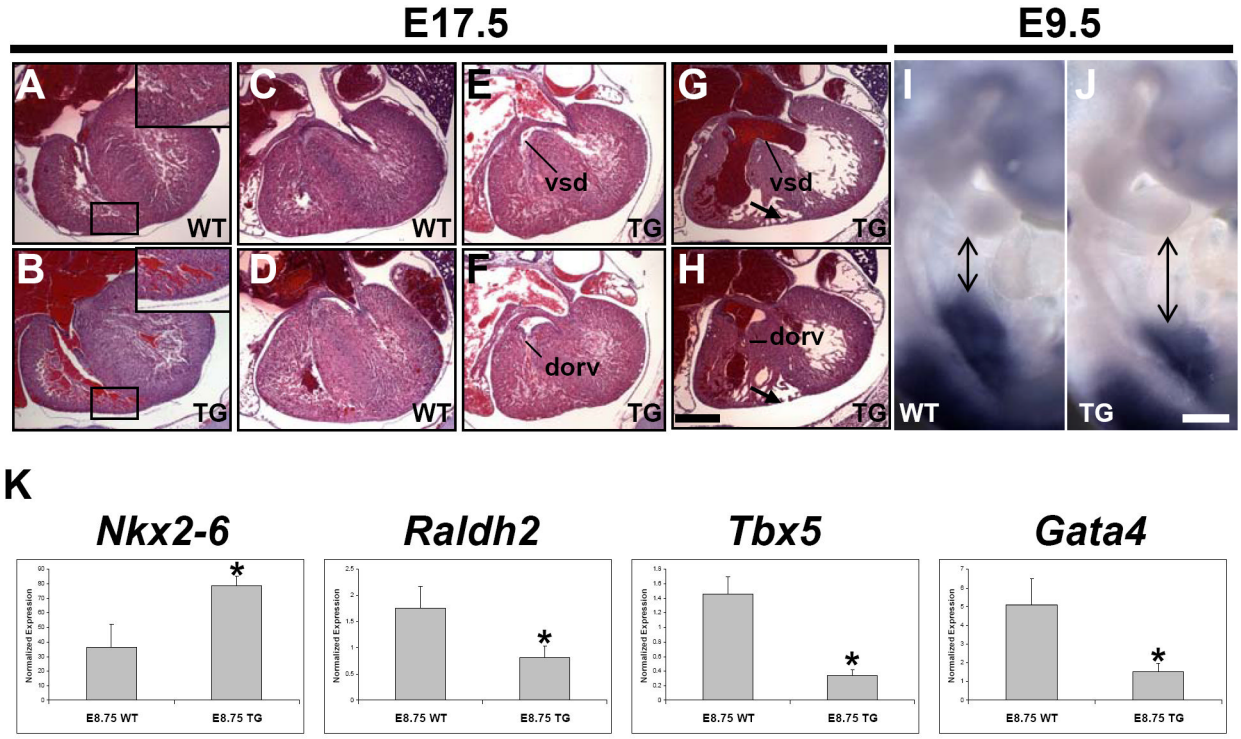

Fig. 5. SHF-derived cardiac defects and opposite gene expression changes in *TBX1* gain-of-function mutants

(A-H)SHF-derived defects in E17.5 BAC transgenic (TG) embryos overexpressing *TBX1* shown by transverse sections. A, C, and D are wild type (WT) embryos. B shows the first BAC transgenic embryo with a thin myocardial wall of the right ventricle (boxed area and magnified in the insets at the top-right of A, B). E and F show ventricular septal defect (vsd) and double outlet right ventricle (dorv) but normal myocardium in the second BAC transgenic embryo. G and H show the third BAC transgenic embryo with ventricular septal defect (vsd), double outlet right ventricle (dorv), and right-ventricular myocardial hypoplasia (black arrow).

(I,J) Whole-mount ISH show *Raldh2*-expressing domain is reduced in the SHF of transgenic embryos (J) compared with wild type embryos (I) at E9.5. Double-headed arrows indicate the relative distance between the cranial border of expression and the caudal border of the first arch.

(K) qRT-PCR analysis of expressions of *Nkx2-6*, *Raldh2*, *Tbx5*, and *Gata4* in BAC transgenic embryos at E8.75. Data displayed here is the mean of at least four independent samples and normalized by *Gapdh* expression. **p*-value<0.01, calculated by two-tailed, unpaired Student's *t*-test. The error bars indicate the standard deviation.

Scale bars: 1 mm in A-H and F-I; 200 μm in I,J.

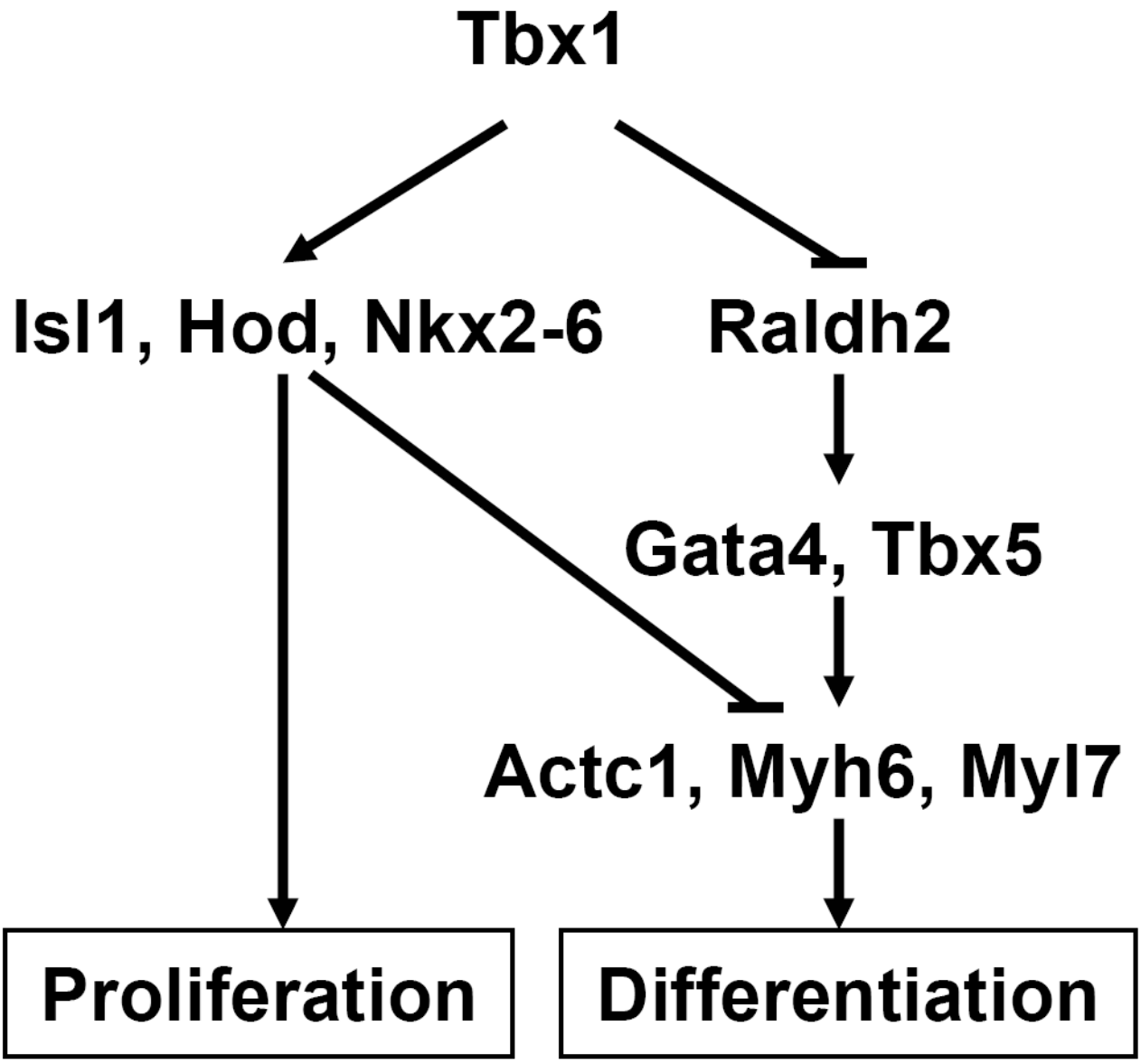

Fig. 6. Model for the regulation of SHF development by *Tbx1* through a genetic Network

Tbx1 maintains the balance between proliferation and differentiation in the SHF by activating *Isl1*, *Nkx2-6*, and *Hod*, while at the same time inhibiting *Raldh2-Gata4/Tbx5-Actc1/Myh6/Myl7* genetic pathway.

Table 1

Selected Tbx1-dependent genes with a potential role in the SHF

Gene symbol	Probe set ID	GenBank ID	E8.75 Fold change	E8.75 *p*-value	E9.75 Fold change	E9.75 *p*-value	E10.75 Fold change	E10.75 *p*-value
Transcriptional regulation								
Ankrd1	1420992_at	AK009959	2.01	0.231	-1.87	0.025	2.81	0.012
Gata4[a,b]	1418863_at	NM_008092	4.48	0.144	3.53	0.013	5.51	0.001
Gata5	1450126_at	BB447551	2.09	0.164	1.59	0.039	3.54	0.002
Gata6	1425463_at	BM214048	-1.07	0.778	1.57	0.077	2.30	0.014
	1425464_at	BM214048	1.38	0.020	1.76	0.003	2.75	0.003
Hod[a,b]	1428662_a_at	AK009007	-2.11	0.000	-1.63	0.015	1.00	0.990
Irx2	1426298_at	AF295369	-2.26	0.030	1.10	0.446	-1.05	0.705
Isl1[a,b]	1422720_at	BQ176915	-2.40	0.001	1.02	0.896	1.07	0.165
Myocd[a]	1425978_at	AF384055	1.01	0.954	1.17	0.674	4.34	0.003
Nkx2-6[a,b]	1452018_at	AF045150	-4.24	0.004	-3.29	0.005	-1.47	0.026
Sox7[a]	1416564_at	NM_011446	2.19	0.009	1.15	0.370	1.80	0.055
T	1419304_at	NM_009309	1.47	0.459	2.24	0.029	1.19	0.303
Tbx5[a,b]	1425695_at	AI425735	2.59	0.161	3.50	0.001	3.57	0.001
Tbx18	1449871_at	NM_023814	1.84	0.108	3.08	0.045	2.48	0.002
Zfpm2[a]	1449314_at	NM_011766	4.47	0.103	2.73	0.003	3.54	0.005
Signaling								
Bmp6[a]	1450759_at	NM_007556	-1.01	0.952	-2.06	0.006	1.28	0.185
Dkk1	1420360_at	NM_010051	-1.52	0.177	-2.10	0.002	-1.46	0.015
Wnt2	1449425_at	BC026373	3.33	0.061	5.01	0.001	5.39	0.006
Wnt11	1450772_at	NM_009519	1.00	0.650	1.25	0.311	2.25	0.016
Muscle contraction								
Actc1[a]	1415927_at	NM_009608	3.01	0.251	1.60	0.021	2.72	0.007
Actg2[a]	1422340_a_at	NM_009610	1.16	0.256	1.19	0.206	2.32	0.024
Actn2	1448327_at	NM_033268	4.27	0.178	-1.46	0.157	2.97	0.012
Cnn1[a]	1417917_at	NM_009922	1.13	0.686	1.33	0.087	2.13	0.024
Mybpc3	1418551_at	NM_008653	2.00	0.308	1.05	0.778	2.29	0.006
Myh6[a,b]	1448826_at	BB481540	3.89	0.271	4.81	0.001	13.53	0.000
Myl4	1422580_at	NM_010858	2.36	0.222	1.05	0.858	7.08	0.004
Myl7[a]	1449071_at	NM_022879	1.80	0.256	1.17	0.327	7.23	0.002
Myom1	1420693_at	NM_010867	1.42	0.497	-1.58	0.006	3.12	0.013
Tnnc1	1418370_at	NM_009393	2.36	0.200	-1.64	0.017	4.13	0.000
Tnni1	1450813_a_at	NM_021467	1.34	0.333	1.20	0.212	3.17	0.006
Tnnt2	1424967_x_at	L47552	1.87	0.279	1.27	0.162	5.85	0.001
Ttn	1427446_s_at	BC025840	2.77	0.322	1.31	0.082	2.45	0.049
Metabolism								
Raldh2[a,b]	1422789_at	NM_009022	2.45	0.035	4.70	0.016	2.11	0.005
Transport								
Cmya1	1419220_at	NM_011724	1.22	0.724	-2.20	0.003	1.12	0.551

Fold change is the average of three replicates. Negative numbers mean downregulation in *Tbx1* null embryos and positive numbers mean upregulation. *p*-value is calculated by Student's t-test. The value is presented as 0.000 when it is less than 0.0005.

[a] validated by qRT-PCR ($p<0.05$).

[b] validated by ISH.